

Colloidal TiO₂-Modified Mesoporous Electron Transport Layer in Perovskite Solar Cells

Evira Bella Yustiani ^a, Putri Nur Anggraini ^b, Shobih ^b, Eri Widiyanto ^c,
Lilis Retnaningsih ^b, Syoni Soepriyanto ^a, Imam Santoso ^a,
Natalita Maulani Nursam ^{b,*}

^a Department of Metallurgical Engineering
Bandung Institute of Technology
Gd. LABTEK IVa Lantai 2, Jl. Ganesha No. 10
Bandung, Indonesia

^b Research Center for Electronics
National Research and Innovation Agency (BRIN)
KST Samaun Samadikun, Jl. Sangkuriang, Dago
Bandung, Indonesia

^c Department of Mechanical Engineering
Singaperbangsa University
Jl. HS. Ronggo Waluyo, Puseurjaya, Telukjambe Timur
Karawang, Indonesia

Abstract

The electron transport layer (ETL) is a crucial part of perovskite solar cells (PSC) as it governs explicitly the charge extraction at the perovskite/ETL interface. In this study, methylammonium lead iodide-based PSCs with an n-i-p structure were fabricated and modified by adding colloidal TiO₂ into the mesoporous TiO₂ film as ETL, aiming to obtain good paste consistency that facilitates the deposition process. The effect of the colloidal TiO₂ addition on the PSC performance was investigated for ETL with different types of TiO₂ particles, i.e., Degussa P25 (the commercial TiO₂ powder comprising anatase, rutile, and amorphous phase) and pure anatase TiO₂. The physical properties of the resulting TiO₂ films were characterized using scanning electron microscopy, while the solar cell performances were analyzed using current-voltage measurement. Despite producing lower performance than the PSC made with commercial paste, the power conversion efficiency (PCE) of the PSCs could be improved with the introduction of a colloidal TiO₂ solution. An optimum condition was observed depending on the type of TiO₂ particle, where the best-performing device was achieved with a colloidal TiO₂ of 0.4 and 0.2 mL for P25 and anatase TiO₂, respectively. The PCE of the PSC with the optimum concentration of TiO₂ colloid increased to approximately 15% for P25 and significantly increased to 4 times for anatase TiO₂, higher than the PCE of the respective samples without any colloid addition. The amount of colloidal TiO₂ in samples with P25 overall had less impact than the samples with anatase TiO₂.

Keywords: TiO₂, electron transport layer, perovskite, solar cell, colloid, power conversion efficiency.

I. INTRODUCTION

Recently, the development of renewable energy has increased rapidly. The solar photovoltaic (PV) will continue to be in demand and become a popular energy source in the future. The reduction in production costs partially promotes the increasing number of implemented solar PV. For instance, around a 74% decrease in the cost of installation of PV mini-grids between 2010 and 2018 has boosted the number of installed PV capacity in Indonesia [1]. In recent years, third-generation solar cell technology has been widely developed mainly due to the low fabrication cost and high efficiency. One of the manifestations of third-generation solar cells is a perovskite solar cell (PSC). Research on PSC has been reported in a large body of literature as it shows a rapid

increase in power conversion efficiency (PCE) from an initial 3.8% in 2009 [2] to 25.7% in 2023 [3]. The high conversion efficiency of PSC is typically achieved using organometal halide methylammonium lead halide perovskite as a light absorber [4]. Many studies have been carried out as efforts to optimize both the constituting materials and the PSC structure. Most of the current research is carried out towards simplifying the fabrication process by minimizing the need to use sophisticated equipment so that the production costs can be suppressed without reducing the power conversion efficiency.

Titanium dioxide (TiO₂) is the most widely used material for the electron transport layer (ETL) in PSCs to date [5]. TiO₂ has three most commonly found crystalline phases, i.e., anatase, rutile, and brookite. Among the three phases, rutile is the most stable phase, while anatase is a metastable phase and tends to transform to rutile at a temperature range of 600–1000 °C, depending on the size of the crystal and the level of purity [6]. Rutile has a slightly lower band gap energy (i.e., 3.02 eV) compared to brookite (3.14 eV) and anatase (3.23 eV) [7]. Thus, it

* Corresponding Author.

Email: natalita.maulani.nursam@brin.go.id

Received: November 3, 2023 ; Revised: December 1, 2023

Accepted: December 8, 2023 ; Published: December 31, 2023

could absorb some portion of light in the area near-infrared region. During the PSC fabrication, careful attention should be paid to the ETL preparation because the quality of ETL and the ETL/perovskite interface properties are some of the determining factors in achieving high PCE values by minimizing the recombination rate to some extent [8]. In high-efficiency PSC devices, an ETL comprising a mesoporous TiO_2 layer is typically accompanied by a compact thin TiO_2 blocking layer underneath [9].

In this contribution, we aim to fabricate PSCs with mesoporous TiO_2 film as ETL. The PSCs were fabricated in a low-cost n-i-p configuration comprising FTO/c- TiO_2 /m- TiO_2 /MAPbI₃/P3HT/carbon. The mesoporous TiO_2 films were prepared via the spin-coating method using diluted TiO_2 pastes containing two types of commercially available TiO_2 particles, i.e., P25 (Degussa) and anatase TiO_2 (Merck). According to the manufacturer's specification, the P25 contains a mixture of anatase (>70%), rutile, and amorphous phases [10]. Additionally, colloidal TiO_2 with various amounts was introduced into the self-prepared TiO_2 pastes to study how it affects the ETL's properties and, ultimately, to investigate their impacts on the PSC's performance. The addition of TiO_2 colloid was aimed at improving both stabilization and consistency since the paste comprised nanoparticles. Such a step is expected to help facilitate the paste deposition process, particularly using the spin-coating technique. This work demonstrates that improved performance could be attained simply via modifications of the solution-processed route, thereby potentially could be developed toward the low-cost fabrication of large-scale PSCs in the future.

II. EXPERIMENTAL

A. Materials

Titanium (IV) oxide anatase (99.8% trace metal basis) was obtained from Merck and Degussa (Evonik) P25. Titanium (IV) isopropoxide, titanium tetrachloride, nitric acid (65%), α -terpineol, triton X-100, lead (II) iodide, N,N-dimethylformamide (DMF, 99.9%), dimethyl sulfoxide (DMSO, 99.9%), poly(3-hexylthiophene), and 2-propanol were purchased from Sigma-Aldrich. Fluorine-doped tin oxide (FTO) substrates (TEC15, 15 ohm/sq) and methylammonium iodide were obtained from Greatcell-Australia, while carbon paste was obtained from Dyenamo-Sweden.

B. Device Fabrication

FTO glass substrates were initially prepared by cutting them into small pieces with a size of 2×1.5 cm. The FTO was then etched following a specified pattern and then washed using ultrasonication in Teepol detergent solution, deionized water, and lastly, in isopropyl alcohol (IPA). Each washing step was carried out for 15 min, and finally, the substrates were dried using a hair dryer. Next, a synthesis method reported by Murakami *et al.* was used to prepare colloidal TiO_2 [11]. In a reflux reactor, 12.5 mL of titanium isopropoxide and 2 mL of IPA were added dropwise into 75 mL of deionized water while stirring. Then, 0.6 mL of nitric acid (65%) was added. The solution was heated at 80 °C

and mixed continuously for 8 h until it turned into a white translucent solution.

The ETL in this experiment comprised two layers, namely compact TiO_2 (c- TiO_2) and mesoporous TiO_2 (m- TiO_2). The c- TiO_2 serves as a blocking layer and was deposited using the chemical bath deposition method. To prepare the c- TiO_2 film, the FTO substrate was immersed in a 40 mM TiCl_4 solution at 70 °C for 30 min. Next, the samples were put into a muffle furnace to undergo an annealing process at a temperature of 500 °C for 30 min. The next step was the deposition of the mesoporous TiO_2 (m- TiO_2) layer. The preparation of the TiO_2 paste initiated the deposition of the m- TiO_2 layer. The TiO_2 pastes were prepared by crushing 0.26 g of various TiO_2 powders using a mortar, then adding a certain amount of colloidal TiO_2 , terpineol, and triton as a binder solution, after which it was stirred until smooth. Prior to use, all the obtained TiO_2 pastes were then diluted in ethanol with a ratio of 1:5. As a comparison, a reference sample was also prepared following the same dilution using commercial TiO_2 paste from Greatcell Solar (the sample is hereafter labeled as TiO_2 -ref). The photographs of the prepared pastes are shown in Figure 1(a). After the dilution, the TiO_2 paste was deposited onto the substrate using a spin-coating method with a rotation speed of 500 rpm for 40 s, followed by annealing at 500 °C for 30 min. The amount of colloidal TiO_2 used during the preparation was varied to 0, 0.2, 0.4, and 0.5 mL, whereas there are two types of TiO_2 powder used, i.e., anatase TiO_2 (Sigma-Aldrich) and P25 (Degussa). Hence, the samples were labeled as anatase- x or P25- x , where x represents the amount of colloidal TiO_2 added.

The perovskite absorber layer used in this study is methylammonium lead iodide (MAPbI₃). The MAPbI₃ solution was prepared following a recipe according to [12], where the deposition was carried out using spin-coating method in a glove box with H₂O level < 0.1 ppm and O₂ level < 30 ppm to prevent the perovskite layer from reacting with the ambient air. The deposition of the perovskite layer was carried out at a rotation speed of 5000 rpm for 30 seconds, and then at the 6th second, toluene was dripped onto the rotating substrate. The films were then heated on a hotplate at 90 °C for 15 min. The next step was the deposition of poly(3-hexylthiophene) (P3HT) as the hole transport layer (HTL). The P3HT was spun-coated with a speed of 5000 rpm for 30 s and then heated on a hotplate at 90 °C for 20 min. This whole process was carried out in an argon-filled glovebox.

The final step of the device assembly was the deposition of carbon as back contact. A low-temperature carbon paste was used as a cathode and deposited using the doctor blade method in ambient air following a pre-

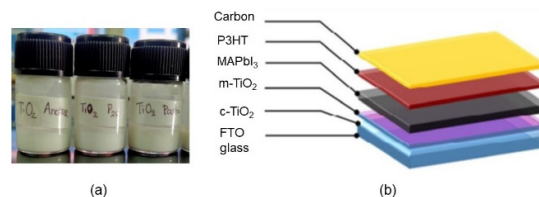


Figure 1. (a) Photograph of the TiO_2 pastes and (b) schematic of the PSC device architecture.

specified pattern. The carbon pastes that had been deposited was then heated at 120 °C for 30 min. Finally, perovskite solar cells with a configuration of FTO/c-TiO₂/m-TiO₂/MAPbI₃/P3HT/C were obtained (Figure 1(b)). The entire device fabrication process is illustrated in Figure 2.

C. Characterizations

Scanning electron microscopy (SEM) images were collected using JEOL JSM IT-300 to analyze the morphology of the samples. The viscosities of the TiO₂ pastes were measured using a Brookfield DV-I+ viscometer. The perovskite solar cells' performance was evaluated by measuring the current density-voltage (J - V) characteristics under a solar simulator equipped with AM 1.5G filter and connected to Keithley 2400 SMU. The incident photon-to-current conversion efficiency (IPCE) was measured using the Newport 2936-R optical power meter.

III. RESULTS AND DISCUSSION

The addition of colloidal TiO₂ into TiO₂ paste may lead to some changes in characteristics, such as paste viscosity and film morphology, which eventually affect the PSC performance. It can be seen from the SEM images shown in Figure 3 (all were taken under 30,000× magnification) that all of the TiO₂ components used during the synthesis herein have different morphologies. Figure 3(a) shows that the TiO₂ P25 is comprised of finely dispersed nanosized particles with a size of around 50 – 70 nm. On the other hand, the anatase TiO₂ exists as spherical aggregates with a size of hundreds of nanometers (Figure 3(b)). Similar to TiO₂ anatase, the powders obtained from colloidal TiO₂ shown in Figure 3(c) also formed agglomerates, although with random sizes. Compared to the rest of the samples, the

commercial TiO₂ paste had the best consistency in particle size and particle density (Figure 3(d)).

The viscosities of the TiO₂ paste were measured to investigate the effect of colloidal TiO₂ addition. The TiO₂ pastes containing either TiO₂ anatase or P25 had similar viscosities, wherein the viscosity was solely determined by the amount of colloidal TiO₂ added into the pastes. The original TiO₂ paste without the addition of colloidal TiO₂ had a viscosity of 11790 cPs, which was still far lower than the viscosity of undiluted commercial TiO₂ paste (i.e., 45290 cPs). The viscosity of the TiO₂ paste was 5033, 2909, and 1787 cPs after being added 0.2, 0.4, and 0.5 mL of colloidal TiO₂, respectively. Since the viscosity of TiO₂ pastes with 0.4 and 0.5 mL of colloidal TiO₂ were substantially low, it should be noted that the TiO₂ deposition for both samples was repeated to achieve thicknesses close to other samples. In general, the viscosity of the paste gradually decreased with the increase in the volume of colloidal TiO₂ added to the paste.

The PSC performance was subsequently studied by measuring the current-voltage (J - V) characteristics under simulated solar irradiation. The J - V curves are shown in Figure 4. The photovoltaic parameters, such as open-circuit voltage (V_{OC}), short-circuit current density (J_{SC}), fill factor (FF), and power conversion efficiency (PCE) were obtained, and the results from the best or champion cells are summarized in Table 1. Meanwhile, the statistical distributions for each parameter are shown in Figure 5. The highest performance with a V_{OC} of 0.55 V, a J_{SC} of 2.22 mA/cm², an FF of 0.30, and a PCE of 0.75% for all modified samples was achieved with P25 that was added with 0.4 mL of colloidal TiO₂. The addition of colloidal TiO₂ in samples with anatase TiO₂ generally has less impact than the samples with anatase TiO₂. For instance, the PCE enhancement for P25 samples ranges between 9

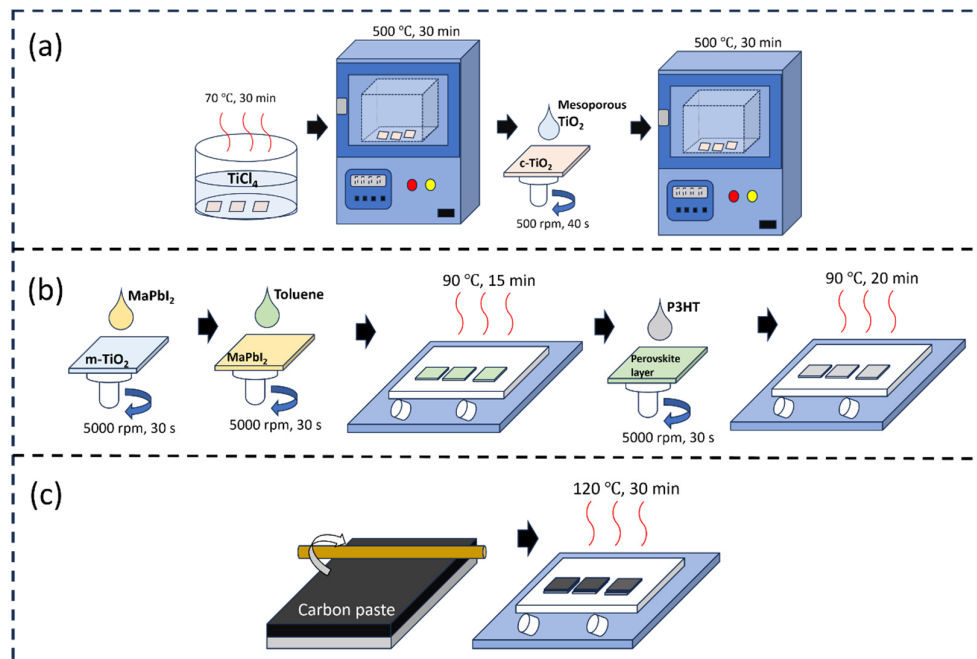


Figure 2. A schematic diagram describing the deposition process of (a) ETL, (b) perovskite layer and HTL, and (c) carbon electrode.

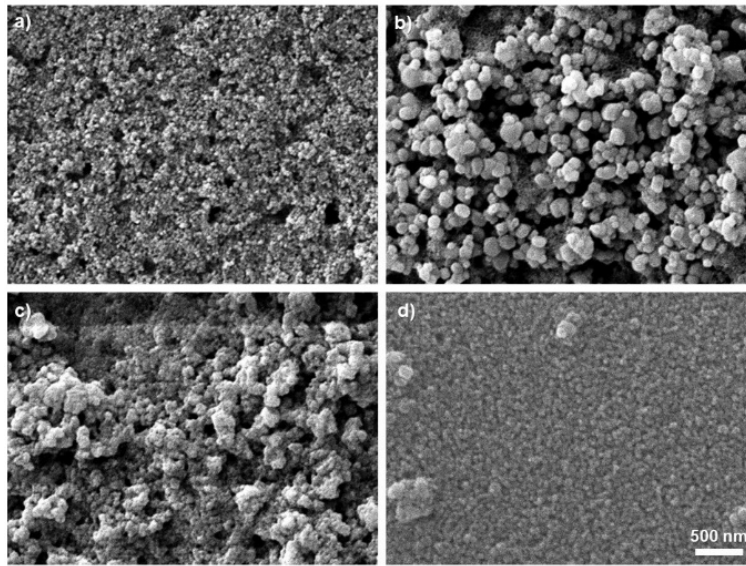


Figure 3. The surface SEM images of (a) P25, (b) anatase, (c) colloidal TiO_2 , and (d) commercial TiO_2 paste (Greatcell Solar). The scale is the same for all images.

and 29% compared to the unmodified sample (i.e., P25-0). However, the PCE of anatase samples showed significant enhancement with an increase of 60% and even more than 3 times higher for the best-performing sample, that is anatase-0.2, compared to the PCE of the unmodified sample. From the morphological perspective, it is likely that the addition of colloidal TiO_2 solution only had an insignificant effect on P25 because it originally had evenly distributed small particle sizes. Meanwhile, since the anatase TiO_2 tends to agglomerate (as evidenced by the SEM image in Figure 3(b)), the addition of colloidal TiO_2 in small amounts promoted the interconnection between the large aggregate, whereas further adding the colloidal did not positively affect the solar cell performance since it may only break the agglomerates without reducing the aggregation of nearby particles. The overall results demonstrate that the addition of colloidal TiO_2 could affect the efficiency of PSCs.

TABLE 1
PHOTOVOLTAIC PARAMETERS OF CHAMPION PSC WITH VARIOUS ETL

Sample	Parameters			
	V_{oc} (V)	J_{sc} (mA/cm^2)	FF	PCE (%)
P25-0	0.63	2.09	0.25	0.65
P25-0.2	0.49	1.76	0.28	0.48
P25-0.4	0.55	2.22	0.30	0.75
P25-0.5	0.46	2.44	0.26	0.57
Anatase-0	0.36	0.88	0.27	0.17
Anatase-0.2	0.57	2.29	0.26	0.69
Anatase-0.4	0.45	1.25	0.24	0.27
Anatase-0.5	0.29	0.69	0.26	0.11
TiO_2 -ref	0.65	3.35	0.28	1.22

The external quantum efficiency that is represented by the measurement of incident photon-to-current conversion efficiency (IPCE) is shown in Figure 5. The

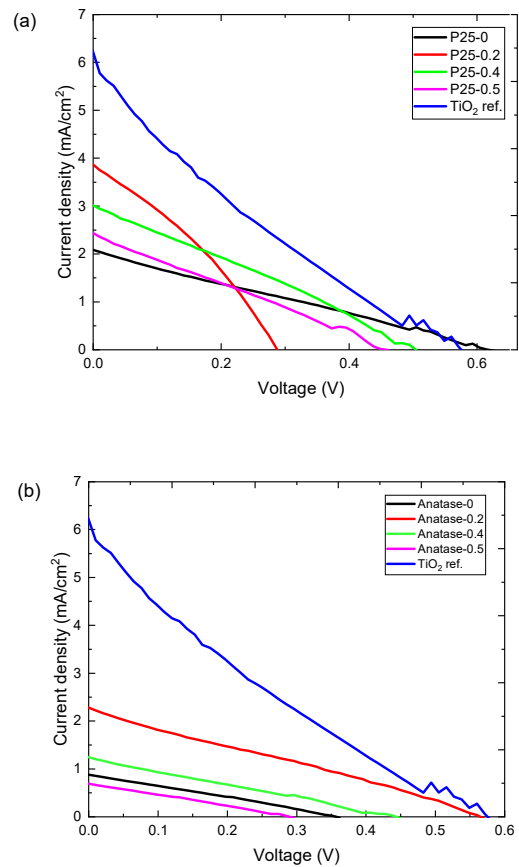


Figure 4. J - V curves for PSCs with various (a) P25 and (b) anatase TiO_2 as ETL.

IPCE of all samples shows broad absorption spectra between 300 to 800 nm, which could be assigned to the absorption band of MAPbI₃. The higher the IPCE value, the greater the number of photons converted into current. Figure 6 shows that the magnitude of IPCE spectra is affected by the amounts of colloidal TiO₂ added. The order of the IPCE intensities was in good agreement with the results obtained in the J - V characterization, where the optimum results were obtained by P25-0.4 and anatase-0.2. This suggests that the absorption of photon and carrier injection are highly influenced by the morphology

of TiO₂ as ETL, which is determined by the presence of colloidal TiO₂.

From both the J - V and IPCE characterization results, all of the PSC samples prepared from either the P25 or anatase TiO₂ show inferior performance compared to the PSC fabricated with commercial TiO₂ (i.e., TiO₂-ref). The best cell fabricated using commercial TiO₂ paste produced a V_{OC} of 0.65 V, a J_{SC} of 3.35 mA/cm², an FF of 0.28, and a PCE of 1.22%. Comparing all parameters, the fill factor is the sole parameter that is rather insensitive to the ETL variation nor the addition of colloidal TiO₂, where the values deviate within around 25%. Both V_{OC} and I_{SC} , on the other hand, are significantly affected by the ETL. High V_{OC} values are achieved by samples with both commercial and P25 TiO₂ without colloidal addition. The V_{OC} is typically influenced by the degree of non-radiative recombination of carriers that could occur in the bulk of the perovskite and at the perovskite interface [13]. Herein, the recombination at the ETL/perovskite interface seems to play a major part in determining the V_{OC} , as the values vary substantially with different ETLs. In the case of P25, adding colloidal TiO₂ reduces the V_{OC} , while there is no consistent trend observed for the samples with anatase TiO₂. A possible explanation is that the lower viscosity induced by the addition of colloidal TiO₂ may have reduced the uniformity of the mesoporous TiO₂ film, hence increasing the defects of the ETL/perovskite interface. Further studies, however, are required to support this assumption. Meanwhile, the J_{SC} is typically

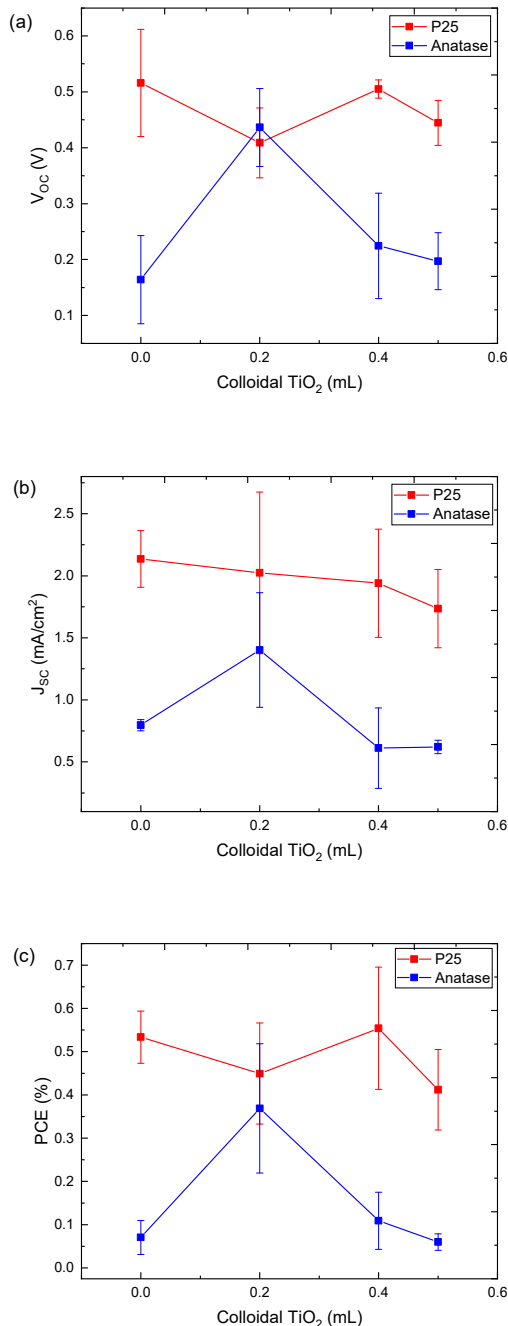


Figure 5. Photovoltaic parameters (a) V_{OC} , (b) J_{SC} , and (c) PCE for PSCs with various ETL.

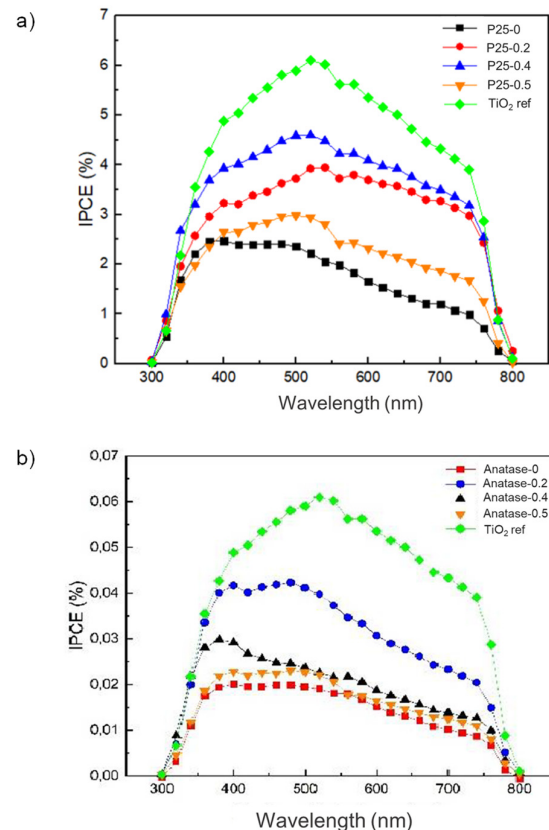


Figure 6. PCE spectra for PSC with (a) P25 and (b) anatase TiO₂.

determined by the perovskite absorber. The quality of the perovskite film could be influenced by the physical properties of the perovskite crystals, wherein large grains with minimum boundaries are favored [14]–[19]. Despite being less affected than V_{OC} , the ETL variation still shows some effect in the J_{SC} , as also confirmed by the IPCE results. In the future, further optimization of interface engineering and modifications involving the TiO_2 compact layer is required to improve the PSC performance.

IV. CONCLUSION

In this study, the effect of TiO_2 powder and the addition of colloidal TiO_2 have been studied on the morphology of the electron transport layer and the performance of PSCs. The PSCs were fabricated with an architecture of FTO/c- TiO_2 /m- TiO_2 /MAPbI₃/P3HT/carbon. The addition of colloidal TiO_2 generally lowers the viscosity of the paste, which eventually affects the morphology of the resulting mesoporous TiO_2 film. The PCE of PSC with P25 and anatase TiO_2 as the ETL reached the optimum condition when added with 0.4 mL (PCE=0.75%) and 0.2 mL (PCE=0.69%) of colloidal TiO_2 , respectively. The PSCs with P25 TiO_2 as ETL, on average, produced superior performance than those with anatase TiO_2 . This work shows that improvement in the quality of the mesoporous TiO_2 layer is essential in affecting the interfacial contact between the TiO_2 and MAPbI₃ active layer.

DECLARATIONS

Conflict of Interest

The authors have declared that no competing interests exist.

CRedit Authorship Contribution

EBY: Investigation, Data Curation, Writing - Original Draft; PNA: Data Curation, Visualization, Writing - Review and Editing; S: Methodology, Investigation, Formal analysis; EW: Data Curation, Formal analysis; LR: Writing - Review and Editing; SS: Supervision, Funding acquisition; IS: Data Curation, Supervision; NMN: Conceptualization, Supervision, Writing - Review and Editing, Funding acquisition.

Funding

Research reported in this publication was supported by Riset dan Inovasi untuk Indonesia Maju (RIIM) funded by LPDP – BRIN and was partially supported by a grant from ITB – PT. Timah, Tbk.

Acknowledgment

The authors thankfully acknowledge support from Metallurgical Engineering ITB and the Advanced Photovoltaic and Functional Electronic Devices research group at the Research Center for Electronics, Badan Riset dan Inovasi Nasional (BRIN). E-layanan Sains (ELSA) BRIN is acknowledged for providing access to the materials characterization.

REFERENCES

- [1] International Renewable Energy Agency, "Future of wind: Deployment, investment, technology, grid integration and socio-economic aspects (A Global Energy Transformation paper)," International Renewable Energy Agency, Abu Dhabi, 2019.
- [2] A. Kojima, K. Teshima, Y. Shirai, and T. Miyasaka, "Organometal halide perovskites as visible-light sensitizers for photovoltaic cells," *J. Am. Chem. Soc.*, vol. 131, no. 17, pp. 6050–6051, Apr. 2009, doi: 10.1021/ja809598r.
- [3] J. Park, J. Kim, H. S. Yun, M. J. Paik, E. Noh, H. J. Mun, M. G. Kim, T. J. Shin, and S. I. Seok, "Controlled growth of perovskite layers with volatile alkylammonium chlorides," *Nature*, vol. 616, no. 7958, pp. 724–730, Feb. 2023, doi: 10.1038/s41586-023-05825-y.
- [4] S. Khatoon, S. K. Yadav, V. Chakravorty, J. Singh, R. B. Singh, M. S. Hasnain, and S. M. M. Hasnain, "Perovskite solar cell's efficiency, stability and scalability: A review," *Int. J. Energy Res.*, vol. 46, no. 15, pp. 21441–21451, Dec. 2022, doi: 10.1002/ER.7958.
- [5] S. Foo, M. Thambidurai, P. S. Kumar, R. Yuvakkumar, Y. Huang, and C. Dang, "Recent review on electron transport layers in perovskite solar cells," *Int. J. Energy Res.*, no. 15, pp. 21441–21451, Dec. 2022, doi: 10.1002/ER.7958.
- [6] A. Yamakata, and J. J. M. Vequizo, "Curious behaviors of photogenerated electrons and holes at the defects on anatase, rutile, and brookite TiO_2 powders: a review," *J. Photochem. Photobiol. C Photochem. Rev.*, vol. 40, pp. 234–243, Sep. 2019, doi: 10.1016/j.jphotochemrev.2018.12.001.
- [7] M. Grätzel and F. P. Rotzinger, "The influence of the crystal lattice structure on the conduction band energy of oxides of titanium(IV)," *Chem. Phys. Lett.*, vol. 118, no. 5, pp. 474–477, Aug. 1985, doi: 10.1016/0009-2614(85)85335-5.
- [8] H. Zhu, Y. Ren, L. Pan, O. Ouellette, F. T. Eickemeyer, Y. Wu, X. Li, S. Wang, H. Liu, X. Dong, S. M. Zakeeruddin, Y. Liu, A. Hagfeldt, and M. Grätzel, "Synergistic effect of fluorinated passivator and hole transport dopant enables stable perovskite solar cells with an efficiency near 24%," *J. Am. Chem. Soc.*, vol. 143, no. 8, pp. 3231–3237, Feb. 2021, doi: 10.1021/jacs.0c12802.
- [9] H. Liu, X. Fu, W. Fu, B. Zong, L. Huang, H. Bala, S. Wang, Z. Guo, G. Sun, J. Cao, Z. Zhang, "An effective TiO_2 blocking layer for hole-conductor-free perovskite solar cells based on carbon counter electrode," *Org. Electron.*, vol. 59, pp. 253–259, Aug. 2018, doi: 10.1016/j.orgel.2018.04.042.
- [10] B. Ohtani, O. O. Prieto-Mahaney, D. Li, R. Abe, "What is Degussa (Evonik) P25? Crystalline composition analysis, reconstruction from isolated pure particles and photocatalytic activity test," *J. Photochem. Photobiol. A: Chem.*, vol. 216, no. 2–3, pp. 179–182, Dec. 2010, doi: 10.1016/j.jphotochem.2010.07.024.
- [11] T. N. Murakami, S. Ito, Q. Wang, M. K. Nazeeruddin, T. Bessho, I. Cesar, P. Liska, R. Humphry-Baker, P. Comte, P. Péchy, M. Grätzel, "Highly efficient dye-sensitized solar cells based on carbon black counter electrodes," *J. Electrochem. Soc.*, vol. 153, no. 12, Art. no. A2255, Oct. 2006, doi: 10.1149/1.2358087.
- [12] E. Widiyanto, Shobih, E. S. Rosa, K. Triyana, N. M. Nursam, I. Santoso, "Graphene oxide as an effective hole transport material for low-cost carbon-based mesoscopic perovskite solar cells," *Adv. Nat. Sci. Nanosci. Nanotechnol.*, vol. 12, no. 3, Art. no. 035001, Sep. 2021, doi: 10.1088/2043-6262/ac204a.
- [13] N. Wu, Y. Wu, D. Walter, H. Shen, T. Duong, D. Grant, C. Barugkin, X. Fu, J. Peng, T. White, K. Catchpole, K. Weber, "Identifying the cause of voltage and fill factor losses in perovskite solar cells by using luminescence measurements," *Energy Technol.*, vol. 5, no. 10, pp. 1827–1835, Oct. 2017, doi: 10.1002/ente.201700374.
- [14] M. Nukunudompanich, G. Budiutama, K. Suzuki, K. Hasegawa, and M. Ihara, "Dominant effect of the grain size of the MAPbI₃ perovskite controlled by the surface roughness of TiO_2 on the performance of perovskite solar cells," *CrystEngComm*, vol. 22, no. 16, pp. 2718–2727, Feb. 2020, doi: 10.1039/d0ce00169d.
- [15] M. I. El-Henaway, I. M. Hossain, L. Zhang, B. Bagheri, R. Kottokaran, and V. L. Dalal, "Influence of grain size on the photo-stability of perovskite solar cells," *J. Mater. Sci. Mater. Electron.*, vol. 32, pp. 4067–4075, Jan. 2021, doi: 10.1007/s10854-020-05148-y.
- [16] Q. An, F. Paulus, D. Becker-Koch, C. Cho, Q. Sun, A. Weu, S. Bitton, N. Tessler, and Y. Vaynzof, "Small grains as recombination hot spots in perovskite solar cells," *Matter*, vol. 4, no. 5, pp. 1683–1701, May 2021, doi: 10.1016/j.matt.2021.02.020.
- [17] Z. Wang and Y. Jiang, "Advances in perovskite solar cells: Film morphology control and interface engineering," *J. Clean. Prod.*, vol. 317, Art. no. 128368, Oct. 2021, doi: 10.1016/j.jclepro.2021.128368.

- [18] H. A. Bioki, A. Moshaii, and M. B. Zarandi, "Improved morphology, structure and optical properties of CH₃NH₃PbI₃ film via HQ additive in PbI₂ precursor solution for efficient and stable mesoporous perovskite solar cells," *Synth. Met.*, vol. 283, Art. no. 116965, 2022, doi: 10.1016/j.synthmet.2021.116965.
- [19] N. Guan, Y. Zhang, W. Chen, Z. Jiang, L. Gu, R. Zhu, D. Yadav, D. Li, B. Xu, L. Cao, X. Gao, Y. Chen, and L. Song, "Deciphering the morphology change and performance enhancement for perovskite solar cells induced by surface modification," *Adv. Sci.*, vol. 10, no. 3, Art. no. 2205342, Dec. 2023, doi: 10.1002/advs.202205342.